

Provided for non-commercial research and education use.
Not for reproduction, distribution or commercial use.



This article was published in an Elsevier journal. The attached copy is furnished to the author for non-commercial research and education use, including for instruction at the author's institution, sharing with colleagues and providing to institution administration.

Other uses, including reproduction and distribution, or selling or licensing copies, or posting to personal, institutional or third party websites are prohibited.

In most cases authors are permitted to post their version of the article (e.g. in Word or Tex form) to their personal website or institutional repository. Authors requiring further information regarding Elsevier's archiving and manuscript policies are encouraged to visit:

<http://www.elsevier.com/copyright>



Interannual variability of smoke and warm cloud relationships in the Amazon as inferred from MODIS retrievals

Hongbin Yu^{a,b,c,*}, Rong Fu^b, Robert E. Dickinson^b, Yan Zhang^b, Mingxuan Chen^b, Hui Wang^b

^a *Goddard Earth Science and Technology Center, University of Maryland at Baltimore County, Baltimore, Maryland, United States*

^b *School of Earth and Atmospheric Sciences, Georgia Institute of Technology, Atlanta, Georgia, United States*

^c *Laboratory for Atmospheres, NASA Goddard Space Flight Center, Greenbelt, Maryland, United States*

Received 29 November 2006; received in revised form 26 March 2007; accepted 1 April 2007

Abstract

Aerosol and cloud data from the MODerate resolution Imaging Spectroradiometer (MODIS) onboard the Earth Observing System (EOS) Aqua are used to investigate interannual variability of smoke and warm cloud relationships during the dry-to-wet transition season (August–October) over the Amazon for two years and its association with meteorological conditions. In one year (2003), smoke aerosols are associated with an increase of cloud fraction and a decrease of cloud effective radius. These effects amplify the cooling at the surface and at the top of the atmosphere (TOA) caused by the aerosol extinction. However, in another year (2002) the cloud fraction decreases with increasing aerosol optical depth. Such a decrease of cloud fraction could offset the effect of increased reflection of solar radiation by the aerosols both at the surface and at TOA. The changes in radiative fluxes between these years would contribute to interannual changes of surface energy fluxes and radiative balance at the top of the atmosphere and influence variability of the wet season onset in the basin. In 2003, the atmosphere was more humid and less stable. These conditions may be relatively favorable for the activation of aerosol particles into cloud condensation nuclei and hence cloud droplets. In 2002, the clouds were less extensive and thinner in a relatively dry atmosphere and presumably dissipated more easily. This study suggests that the aerosol-cloud relation can be influenced by atmospheric structure and convective motions, in addition to changes in aerosols properties. An adequate characterization of aerosol-cloud relationship would require a longer time series of data that includes a variety of climate conditions. The caveat of this analysis is that differences in aerosol absorption and its vertical distribution may have contributed to the observed interannual change of smoke-cloud relationship but could not be determined due to lack of adequate measurements.

© 2007 Elsevier Inc. All rights reserved.

Keywords: Aerosols; Cloud; Satellite remote sensing

1. Introduction

Biomass burning emits aerosols into the atmosphere. The composition and amount of these aerosols depends on meteorological and biospheric conditions as well as on human activities. In the dry season of the Amazon basin, biomass burning increases the aerosol loading to number concentrations at least several times larger than those in the wet season (Andreae et al., 2004; Roberts et al., 2003). This paper provides observations as to how this smoke aerosol relates to, and

presumably modifies the fractional coverage and droplet size of Amazon warm clouds, and how aerosol-cloud relationship varies with interannual changes of the large-scale meteorological background and aerosols.

Aerosol-cloud relationships are determined by multiple complex, correlated or competing processes. Specifically, aerosol can act as cloud condensation nuclei (CCN), thus increase the number and decrease the size of cloud droplets (Feingold et al., 2001; Kaufman & Fraser, 1997; Twomey, 1977). These changes consequently increase the cloud reflectivity through more scattering (Twomey, 1977). On the other hand, the increase of cloud reflectivity could also be compensated by enhanced cloud absorption in the presence of smoke particles (Kaufman & Nakajima, 1993; Twomey, 1977), a broadening of the droplet size spectrum (Liu & Daum, 2002), and small scale dynamic

* Corresponding author. NASA Goddard Space Flight Center, Code 613.2, Greenbelt, MD 20771, United States. Tel.: +1 301 614 6209; fax: +1 301 614 6307.

E-mail address: hyu@climate.gsfc.nasa.gov (H. Yu).

feedbacks (Jiang et al., 2002). The number of smoke particles activated into CCN depends not only on aerosol size (Dusek et al., 2006) and composition (Charlson et al., 2001; Nenes et al., 2002a) but also on the magnitude of updraft velocities (Feingold et al., 2003; Leaitch et al., 1996), low-tropospheric stability (Matsui et al., 2004), and increase of saturation vapor pressure with aerosol heating (Conant et al., 2002; Nenes et al., 2002b).

Smaller cloud droplets have longer lifetimes and may not grow large enough to precipitate through warm rain processes (Rosenfeld, 1999; Rosenfeld & Lansky, 1998). These effects tend to increase liquid water content (Albrecht, 1989). The suppression of warm rain can promote vertical transport of water and pollutants to the upper troposphere, observed as “smoking clouds” (Andreae et al., 2004), and enhance vertical exchange of water vapor (Sherwood, 2002).

Absorption by smoke cools the surface and heats the atmosphere (Hobbs et al., 1997; Penner et al., 1992; Procopio et al., 2004), changing the surface fluxes and atmospheric thermal and moisture structure (Yu et al., 2002). This effect tends to reduce cloud cover and liquid water path (Ackerman et al., 2000; Feingold et al., 2005; Johnson et al., 2004; Koren et al., 2004), competing with the aerosol effect on cloud microphysics. Thus, whether smoke or pollution aerosol increases or decreases the cloud fraction may depend on magnitude of aerosol absorption (Kaufman & Koren, 2006).

How smoke interacts with the atmospheric boundary layer and clouds depends on the (highly variable) vertical profile of smoke aerosols (Feingold et al., 2005; Johnson et al., 2004; Yu et al., 2002). Different air trajectories may provide different sources of aerosols with distinct size distributions and chemical composition that influence clouds differently (Feingold et al., 2003).

Observed smoke–cloud relationship will vary depending on which of the aforementioned processes dominate as a result of aerosols and meteorological conditions. To understand what controls such variations, we first need to characterize the conditions that lead to changes of aerosol–cloud relationship. To do so, large samples of observations under variety of aerosol, clouds and meteorological conditions have to be used. In-situ measurements can provide more comprehensive and detailed measurements of these conditions, but they are limited in time and space. Satellite remote sensing provide large samples for broad variety of meteorological, aerosols and cloud conditions globally over multiple years, although the measurements are limited to few variables, and generally with greater uncertainty. In this study, we use the MODerate resolution Imaging Spectroradiometer (MODIS) on board of Aqua satellite of the Earth Observing System (EOS) to examine the variations of aerosol–cloud relationship during the peak of biomass burning seasons (August–October) of 2002 and 2003. We also discuss implications of the smoke–cloud relationships and their influence on the radiative budget.

2. Data and methods

2.1. Description of MODIS aerosol and cloud data

MODIS has 36 spectral bands, good spatial resolution of 250–500 m, and nearly global coverage on a daily basis

(Salomonson et al., 1989). Thus, it provides a state-of-art satellite observation of aerosol and cloud radiative properties. Aqua was launched in May 2002 and has an overpass of around 1:30 pm local time when continental warm clouds may be well developed. This timing allows a better detection of smoke–cloud interactions than that of the morning overpass of Terra, another EOS satellite also carrying MODIS. We use the daily MODIS/Aqua Level 3 atmospheric product (i.e., MYD08_D3) aggregated to a spatial resolution of $1^\circ \times 1^\circ$ that includes retrievals of aerosol, cloud, and atmospheric profiles of temperature and moisture (King et al., 2003).

The MODIS aerosol retrieval algorithms and products provide a daily retrieval of aerosols over both ocean and less reflective land regions and at a spatial resolution of 10 km, based on data at a resolution of 500 m (Kaufman et al., 1997; Remer et al., 2005; Tanré et al., 1997). The dark-target method has been successfully used to derive aerosol optical depths at 470 nm and 650 nm over vegetated land under cloud-free conditions (Kaufman et al., 1997; Remer et al., 2005). The derived over-land Ångström exponent is not as reliable as that over ocean (Remer et al., 2005). The Level 2 aerosol retrievals at 10-km pixels (i.e., MYD04) are then aggregated to $1^\circ \times 1^\circ$ grids, generating the Level 3 daily aerosol product included in MYD08_D3.

MODIS uses multiple spectral bands to detect clouds at individual pixels with resolutions of 250 m and 1 km (Platnick et al., 2003), and for the overcast pixels to infer cloud top pressure and temperature (from thermal bands) and droplet effective radius (weighted toward cloud top), columnar optical depth, and water path for different cloud thermodynamic phases (i.e., water, ice, and mixed) at 1 km resolution. These pixel or Level 2 products (i.e., MYD06) are aggregated at 1° spatial resolution on a daily basis, producing Level 3 products including the fraction of cloudiness (King et al., 2003).

The MODIS estimated effective cloud drop radii are used here not for their absolute values but for their variation with aerosol loading. Estimation of cloud average effective radii would require downward correction for two biases: i) the observed values are weighted toward cloud top where updrafts usually promote larger particles; ii) the plane parallel model for radiative transfer used by MODIS consistently overestimates the individual droplet size by 25%–50% (Kaufman & Nakajima, 1993; Marshak et al., 2006; Nakajima et al., 1991; Platnick & Valero, 1995; Rawlins & Foot, 1990; Reid et al., 1999). However, it is reasonable to expect that errors in the observed relative changes of effective radii are small (Nakajima et al., 1991).

2.2. Description of meteorological data

This analysis also uses an atmospheric stability parameter, referred to as lifted index (LI) that is retrieved by MODIS, large-scale meteorological parameters such as wind speed and relative humidity from the European Centre for Medium-Range Weather Forecasts (ECMWF), and operational radiosonde measurements of temperature and moisture in the region. The LI is defined as the ambient air temperature at 500 mb minus the temperature of an air parcel if it convects dry adiabatically from

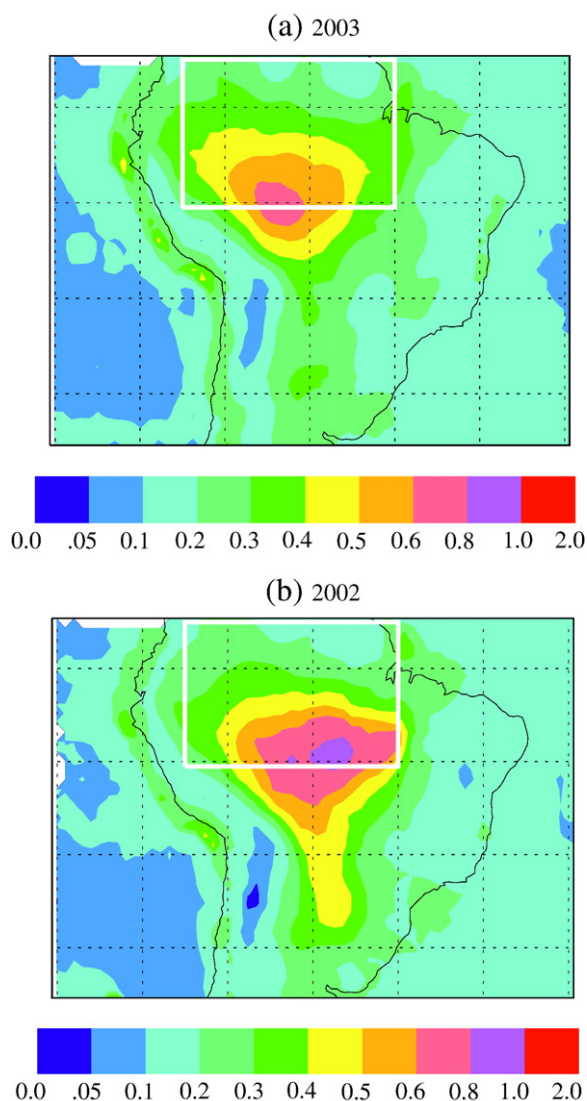


Fig. 1. Distributions of Aqua MODIS aerosol optical depth at 550 nm averaged over August–October of (a) 2003 and (b) 2002. The white box (10°S to 5°N , 50°W to 75°W) illustrates a region selected for smoke-cloud analysis where the land cover is mostly categorized as tropical evergreen broadleaf forest.

the surface to the lifting condensation level and then moist adiabatically to 500 mb level. It is more positive for greater stability (lifted parcels relatively cool compared to environment). Note that MODIS derives the lifted index from the retrieved temperature and humidity profiles under clear-sky conditions. Thus, it is more reliable in representing the atmospheric conditions controlling the formation of warm clouds, which are the focus of this study, than in representing the atmospheric conditions in the vicinity of convection.

Amazon convection can be either predominantly a maritime-type in the wet season or continental-type in the dry season (Peterson et al., 2002; Silva Dias et al., 2002), which have distinct thermal structure and properties of their convection and precipitation. The occurrence of these types is diagnosed by the sign of the low-level meridional wind over northwest Amazon (5°S to 5°N , 65°W to 75°W) (Peterson et al., 2006), referred

to as the V-index (Wang & Fu, 2002). This daily V-index is derived from ECMWF forecast products. Southerly winds would advect smoke aerosols northward from the southern Amazon where biomass burning peaks, whereas northerly winds would bring in relatively pristine air from the rainy northern Amazon.

Vertical wind shear, relative humidity, and water vapor concentration in the lower troposphere are obtained from routine radiosonde measurements. Relative humidity is also obtained from ECMWF forecast products.

2.3. Methods of data analysis

The potential influences of smoke on warm clouds are examined for 2002 and 2003 for the tropical Amazon domain (10°S to 5°N , 75°W to 50°W — shown as a white box in Fig. 1). The later year was “normal,” whereas 2002 was drier. The latter year has been often associated with an El Niño (Hastenrath & Heller, 1977). The domain covers a largely tropical rainforest so that influences of land surface heterogeneity should be small. The distribution of MODIS AOD at 550 nm averaged over August–October of 2003 (Fig. 1a) is similar to that of 2002 (Fig. 1b), but the peak value in the central Amazon for 2003 is only ~ 0.6 , and that for 2002 is as large as 0.9.

Data are selected where there have been more than 10 successful Level 2 ($10\text{ km} \times 10\text{ km}$) aerosol retrievals in a $1^{\circ} \times 1^{\circ}$ grid, where the cloud-top temperature is greater than 273 K (limiting the analysis to warm clouds), and where the V-index is southerly (about 2/3 of the time as seen in Fig. 2), giving in 2002 and 2003 about 4560 and 11,700 data samples, respectively. The $1^{\circ} \times 1^{\circ}$ data are averaged to a grid of $3^{\circ} \times 3^{\circ}$ to remove small-scale dynamical effects and to minimize potential effects of the lack of collocation of aerosol (retrieved under clear sky only) and cloud (Sekiguchi et al., 2003).

We use MODIS aerosol optical depth (AOD) at 550 nm as a proxy of aerosol loading. Heavy biomass burning events with AOD greater than one are excluded because of insufficient sampling. Values of AOD between zero and one are divided into nine bins with a half-width of 0.1 for the first AOD bin

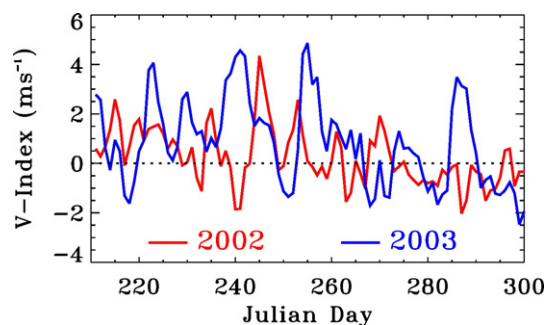


Fig. 2. Comparisons of monsoon index (i.e., V-index) in the Amazon basin between 2002 and 2003. The V-index is defined as the ECMWF daily meridional wind at 925 mb level and averaged over the domain (5°S – 5°N , 65°W – 75°W). A positive and negative value respectively denotes southerly and northerly cross-equatorial flow regime.

(AOD<0.20) and 0.05 for others. Cloud microphysical and optical parameters for cloud optical depth greater than 2 are sorted into individual AOD bins, and for each bin their means and standard errors (i.e., $\sigma/(n-1)^{1/2}$, where σ and n are standard deviation and the number of data points, respectively), are then calculated. The exclusion of high AOD events and low cloud optical depths can also help to reduce possible misclassification of aerosols and clouds and the resulting artificial bias in relating clouds to aerosols (Brennan et al., 2005). The exclusion of optically thin clouds also reduces surface contamination in cloud retrievals. The cloud parameters in the lowest AOD bin ($0 < \text{AOD} < 0.2$) characterize relatively unpolluted clouds as supported by measured aerosol variations both from ground (Procopio et al., 2004) and satellite (Yu et al., 2003).

The data are also stratified by: i) cloud liquid water path (LWP) and cloud-top temperature (T_{cld}) to factor out the dependences of cloud effective radius or cloud fraction on these terms (Feingold et al., 2003; Lohmann & Lesins, 2003; Schwartz et al., 2002); ii) various meteorological parameters, i.e. the MODIS/Aqua retrieved lifted index, ECMWF relative humidity, and a vertical wind shear in the lower troposphere. For brevity, we will not show figures with no clear aerosol-cloud correlations, although all the analysis has been conducted for both years.

3. Results

3.1. Different relation between smoke and clouds in 2002 and 2003

3.1.1. A normal year (2003)

The large-scale meteorological conditions during the period of August–October 2003 were more close to those of an average transition/biomass burning season. Fig. 3 shows for this period the change of cloud-top effective radius (r_{eff}) with increasing aerosol optical depth for different ranges of cloud-top temperature and liquid water path. Fig. 3(d) shows the radius averaged over all ranges of T_{cld} and LWP as a black line. For a clean background atmosphere (i.e., $\text{AOD} < 0.2$), the cloud effective radius clearly increases with increasing liquid water path. Such LWP-dependence of droplet size becomes weaker and hence less certain with greater aerosol optical depths. The droplets in optically thin clouds ($\text{LWP} \leq 40 \text{ gm}^{-2}$) have no obvious change with AOD (data points are limited). Conversely, for thicker clouds ($\text{LWP} > 40 \text{ gm}^{-2}$), the droplet size decreases significantly as aerosols increase from light to medium loading ($\text{AOD} < 0.4-0.6$). This slope is more negative for thicker clouds ($\text{LWP} \geq 70 \text{ gm}^{-2}$). At higher AODs, the droplet size levels off (for $T_{\text{cld}} < 289 \text{ K}$) or slightly increases (for $T_{\text{cld}} > 289 \text{ K}$) with AOD. Fig. 4 shows that cloud optical depth increases with AOD

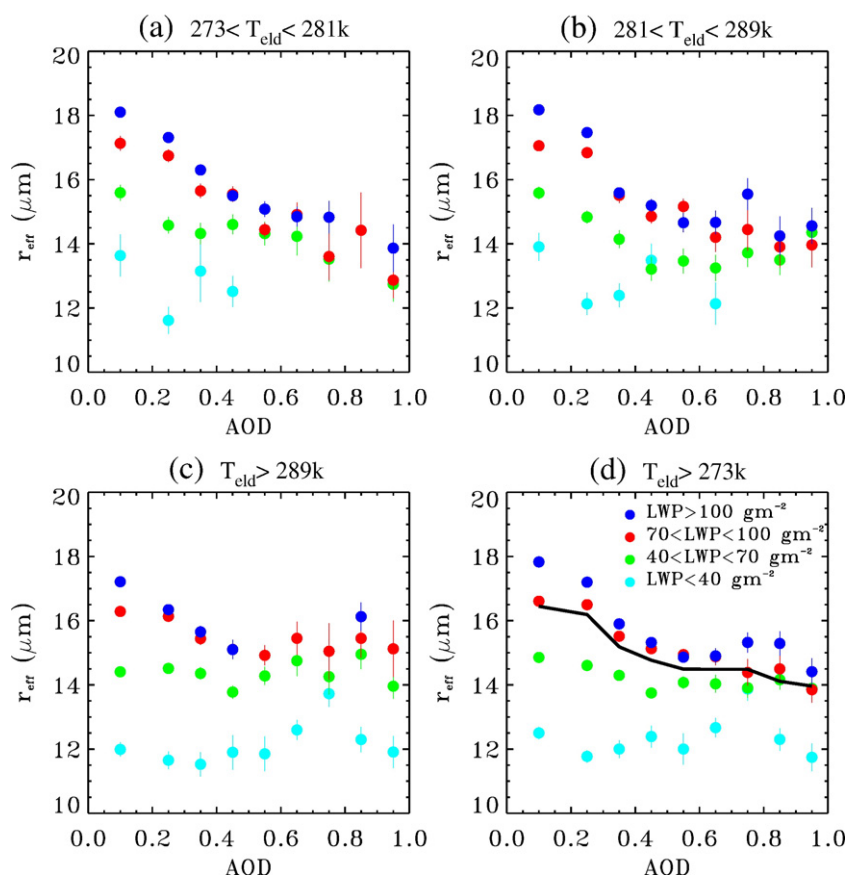


Fig. 3. Cloud-top effective radius (r_{eff}) versus aerosol optical depth (AOD) in 2003. The data are stratified by liquid water path (LWP) for three cloud-top temperature (T_{cld}) categories in (a) to (c). d summarizes for all warm-cloud temperatures. The black line denotes the overall changes for all ranges of LWP and T_{cld} . The averages for individual AOD bins are shown as dots and standard errors as vertical bars.

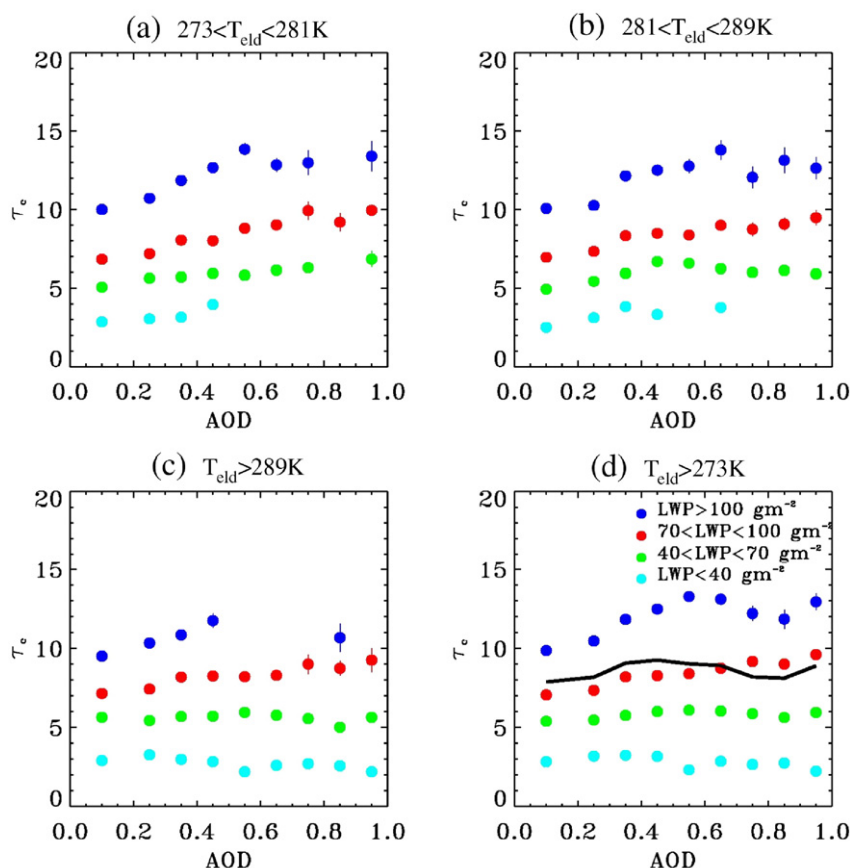


Fig. 4. As in Fig. 3, but for water cloud optical depth (τ_c) versus aerosol optical depth (AOD) in 2003.

when LWP is greater than 70 gm^{-2} . Because such a change is observed for warm clouds with similar LWP, it must be at least in part contributed to by large reductions of cloud effective radius as shown in Fig. 3.

Fig. 5 shows for this period the variation of the warm cloud fraction with aerosol optical depth. Note that the cloud fraction used in this study was derived from MOD06 and aggregated into liquid water cloud category. Its slope is positive for larger liquid water paths and on average for

AOD < 0.6. The thinner clouds (i.e., $\text{LWP} < 70 \text{ gm}^{-2}$) have little slope for AOD < 0.6 but a negative slope for higher AOD conditions. For high aerosol loading (AOD > 0.6), the total cloud fraction is essentially unchanged with AOD, because of the increase of cloud fraction with AOD for higher LWP compensating the decrease of cloud fraction with AOD for lower LWP.

Figs. 3–5 show clearly a decrease of the effective droplet sizes and increase of the optical depths and fractions of clouds

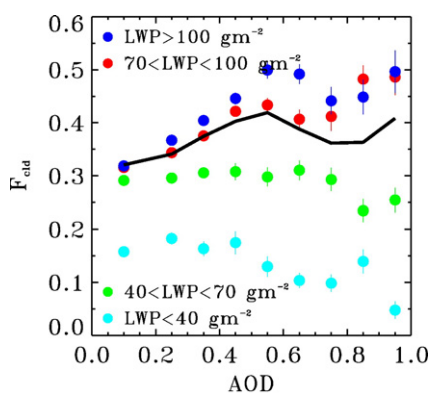


Fig. 5. Cloud fraction (F_{eld}) versus aerosol optical depth (AOD) in 2003, for warm clouds stratified with liquid water path (LWP). The black line denotes the overall change for all ranges of LWP.

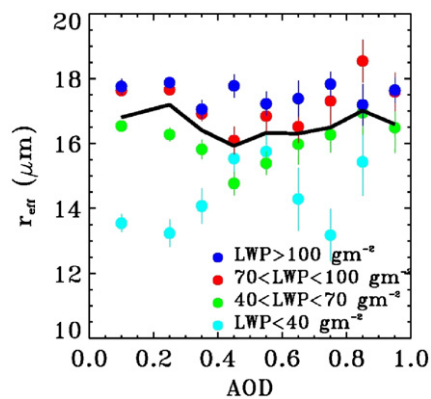


Fig. 6. Cloud-top effective radius (r_{eff}) versus aerosol optical depth (AOD) in 2002. The data are stratified with liquid water path (LWP) and the black line denotes the overall changes for all ranges of LWP.

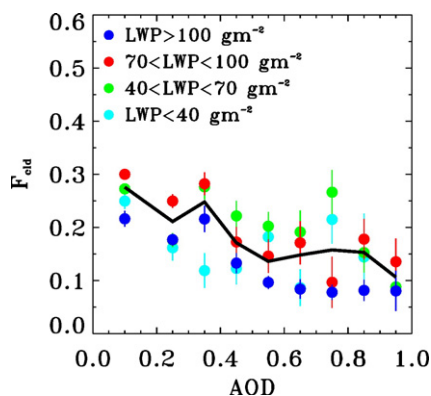


Fig. 7. Cloud fraction (F_{cld}) versus aerosol optical depth (AOD) in 2002. The data for all warm clouds are stratified with liquid water path (LWP). The black line denotes the overall change for all ranges of LWP.

with high LWP ($> 70 \text{ gm}^{-2}$) when AOD increases up to 0.6. The effective droplet sizes and optical depth for clouds with low LWP ($< 40 \text{ gm}^{-2}$) remain unchanged, but cloud fraction decreases with aerosol optical depth. For medium LWP ($40\text{--}70 \text{ gm}^{-2}$), these cloud parameters do not change with aerosol loading.

3.1.2. A dry year (2002)

The atmosphere was drier over the Amazon domain in this El Niño year. The AOD was overall higher and the averaged LWP was smaller. The cloud droplet size does not change significantly with increasing aerosol optical depth, as shown in Fig. 6. The further stratification with cloud-top temperature, similar to that in Fig. 3, does not result in any clearer correlation and is not shown here. The cloud fraction generally decreases with increasing AOD (Fig. 7). For high LWP ($> 100 \text{ gm}^{-2}$) in particular, it decreases from about 0.22 to 0.08, as AOD increases from 0.1 to 0.95. Larger such changes were observed using data with a much higher (10 km) spatial resolution (Koren et al., 2004).

Fig. 8 suggests that cloud top heights decrease as aerosol increases. As AOD increases from 0.1 to 1.0, the cloud-top temperature increases by about 3 K (Fig. 8a), but the clear-sky

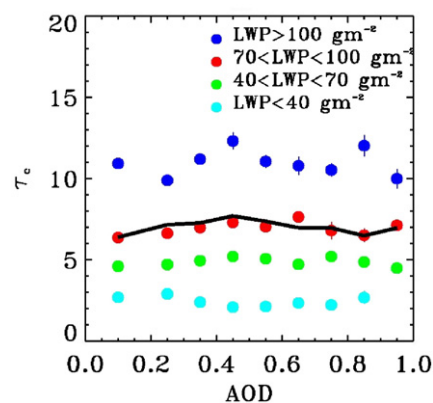


Fig. 9. Water cloud optical depth (τ_c) versus aerosol optical depth (AOD) in 2002. The data are stratified with liquid water path (LWP) and the black line denotes the overall changes for all ranges of LWP.

air temperatures in the lower and middle troposphere increase by less than 1 K (Fig. 8b). Cloud optical depths, on the other hand, do not appear to change with AOD (Fig. 9).

To summarize, we have observed from MODIS different relationships between biomass burning smoke and warm clouds during the dry-to-wet transition season over the Amazon in two different years. Warm clouds were thicker and more extensive in 2003 and showed a decrease of cloud droplet size and an increase of cloud optical depth with increasing aerosol optical depth. The cloud fractions generally increased with aerosol except for clouds that were optically thin or with heavy smoke conditions. In 2002, an El Niño year, aerosol optical depth was higher and the cloud was overall thinner and less extensive. The cloud fractions decreased, and the cloud top temperatures increased with an increase of AOD. Changes of cloud droplet size and optical depth with increasing AOD were not discernable.

The analysis described above has examined smoke-cloud relationships in the southerly regime. No clear smoke-cloud relationship can be detected in the northerly regime (which occurred about 1/3 of the time during the transition season), presumably because of insufficient samples with smoke (Wang & Fu, 2002).

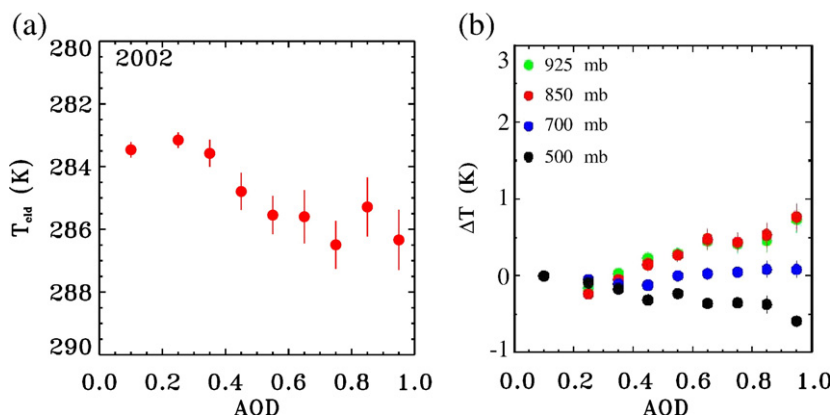


Fig. 8. a) Cloud-top temperature (T_{cld}) of warm clouds versus aerosol optical depth (AOD) in 2002. b) Changes of clear-sky air temperatures with AOD from that of clean air ($\text{AOD} < 0.2$) at various pressure levels in the lower and middle troposphere derived from MODIS.

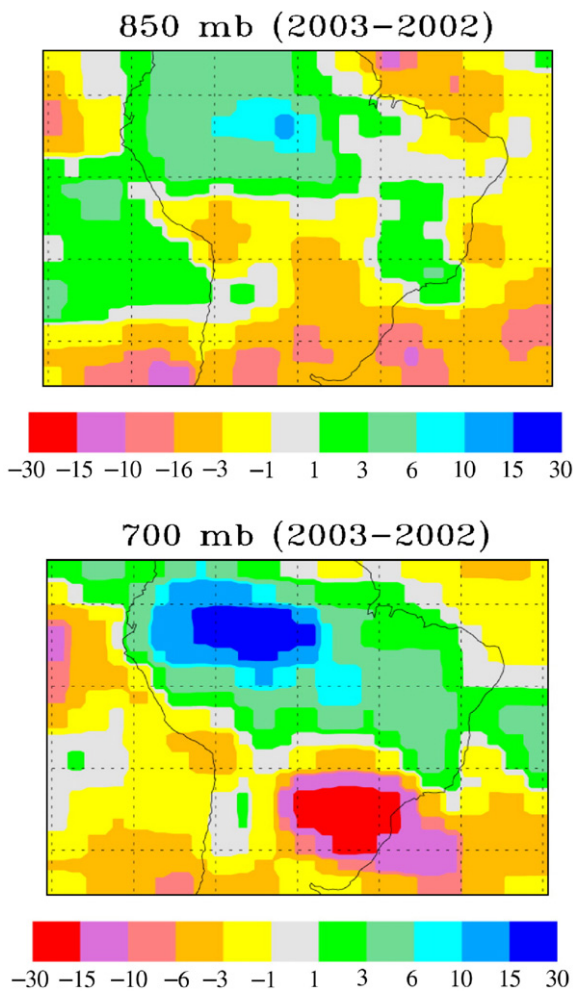


Fig. 10. Change of relative humidity (RH) at 850 mb (left) and 700 mb (right) levels between 2003 and 2002 for August–October seasonal average derived from ECMWF.

3.2. Atmospheric differences between 2002 and 2003

Fig. 10 shows that relative humidity (RH) at 850–700 mb from ECMWF was lower by 5–25% in 2002 than in 2003 in the domain. Likewise, radiosonde observations over Manaus (3.15 °S, 59.98 °W), Brazil, (Fig. 11) show 2002 to be lower by about 10% below 2.5 km and more so above the 2.5 km altitude. The specific humidity in 2002 was also lower by about 1 g kg^{-1} .

Both radiosonde measurements and the MODIS-derived lifted index suggest that the atmosphere was less stable during the transition/biomass burning season in 2003 than in 2002. Fig. 12 shows the profiles of potential temperature (θ), pseudo-equivalent potential temperature (θ_e), and saturated pseudo-equivalent potential temperature (θ_{es}) derived from sounding measurements over Manaus, Brazil. A parcel rising from the near-surface with θ_{e0} has negative buoyancy before intersecting with θ_{es} . Its vertical integral, or the area between the vertical θ_{e0} line (conserved during the lifting) and θ_{es} , is referred to as the convective inhibition negative energy (CINE). After the intersection, the parcel is positively buoyant and can freely rise until $\theta_{e0} = \theta_{es}$ again. The vertical integral of positive buoyancy is called convective available potential energy (CAPE). Fig. 12 shows a smaller CINE and larger CAPE in 2003 than 2002, implying a conditionally more unstable atmosphere.

Fig. 13(a) shows the frequency of occurrence of MODIS-derived lifted index for aerosol optical depth of less than 0.2, i.e., a proxy for pristine background. Clearly, in the tropical Amazon, the LI peaked at ~ 1.5 (less stable) in 2003, while it was more like ~ 3 (more stable) in 2002. In 2003, the LI was more often less than 0 (i.e., unstable), compared to 2002. The average LI was about 1.4 in 2003, much smaller than the 3.9 in 2002. Thus, the MODIS LI indicates that the atmosphere was less stable in 2003 than in 2002.

Fig. 13 also shows the distribution function of liquid water path (b), warm cloud fraction (c), and cloud optical depth (d), all for $\text{AOD} < 0.2$ (a proxy for background condition). The

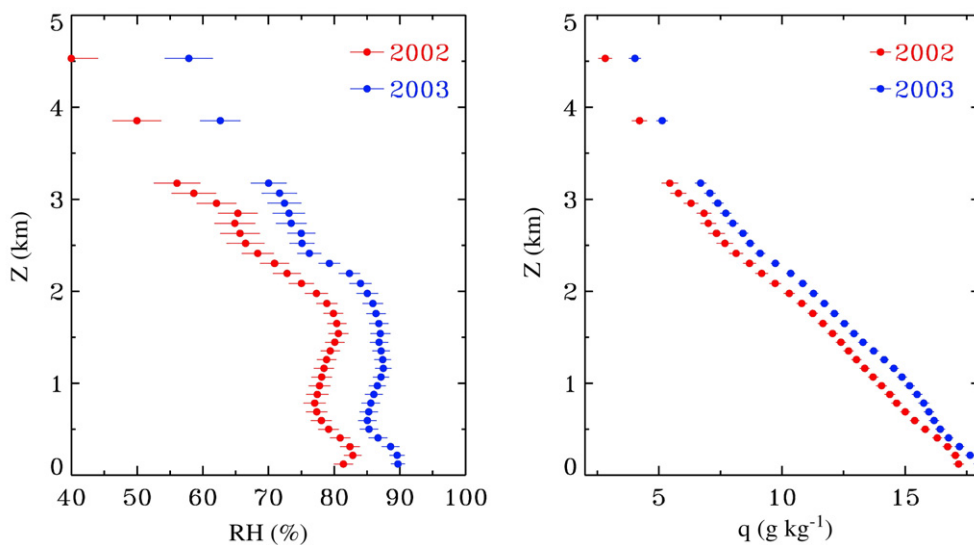


Fig. 11. Relative humidity (RH) and specific humidity (q) profiles for 2002 (red) and 2003 (blue) derived from radiosonde measurements over Manaus (3.15 °S, 59.98 °W), Brazil.

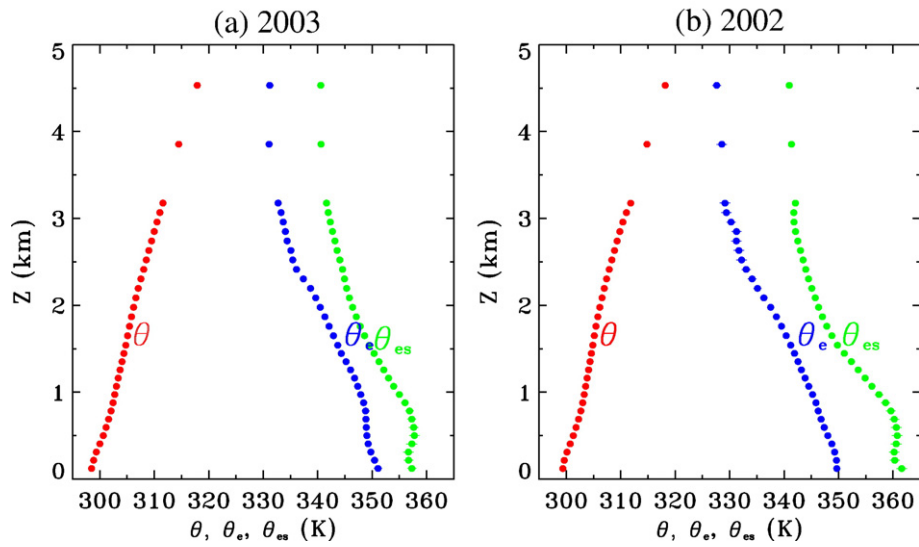


Fig. 12. Comparisons of 2003 (a) and 2002 (b) radiosonde profiles of potential temperature (θ , red), pseudo-equivalent potential temperature (θ_e , blue), and saturated pseudo-equivalent potential temperature (θ_{es} , green) over Manaus (3.15 °S, 59.98 °W), Brazil.

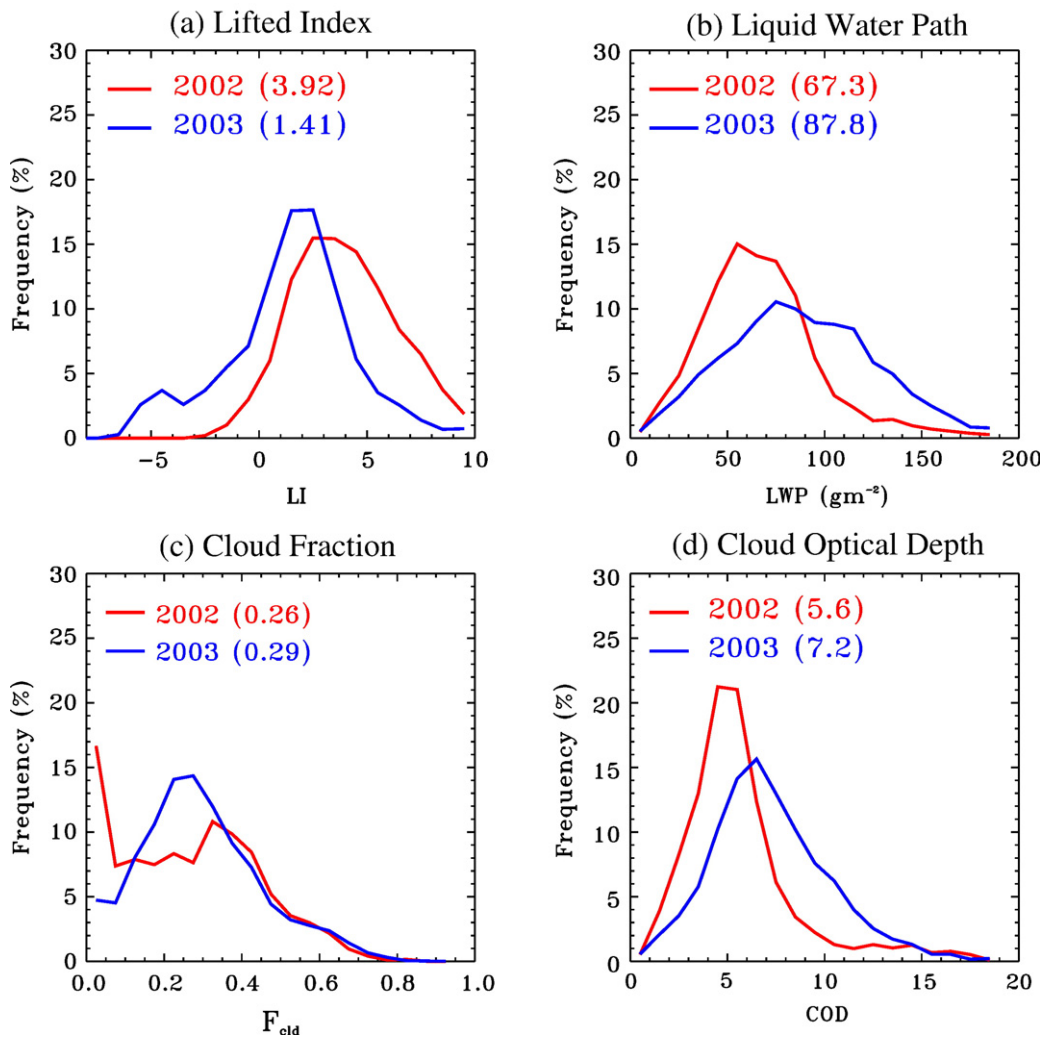


Fig. 13. Distribution of (a) lifted index, (b) liquid water path, (c) warm cloud fraction, and (d) cloud optical depth for aerosol optical depth less than 0.2, i.e., a proxy of clean background condition. Blue and red denotes 2002 and 2003 respectively. Numbers in parentheses are average values.

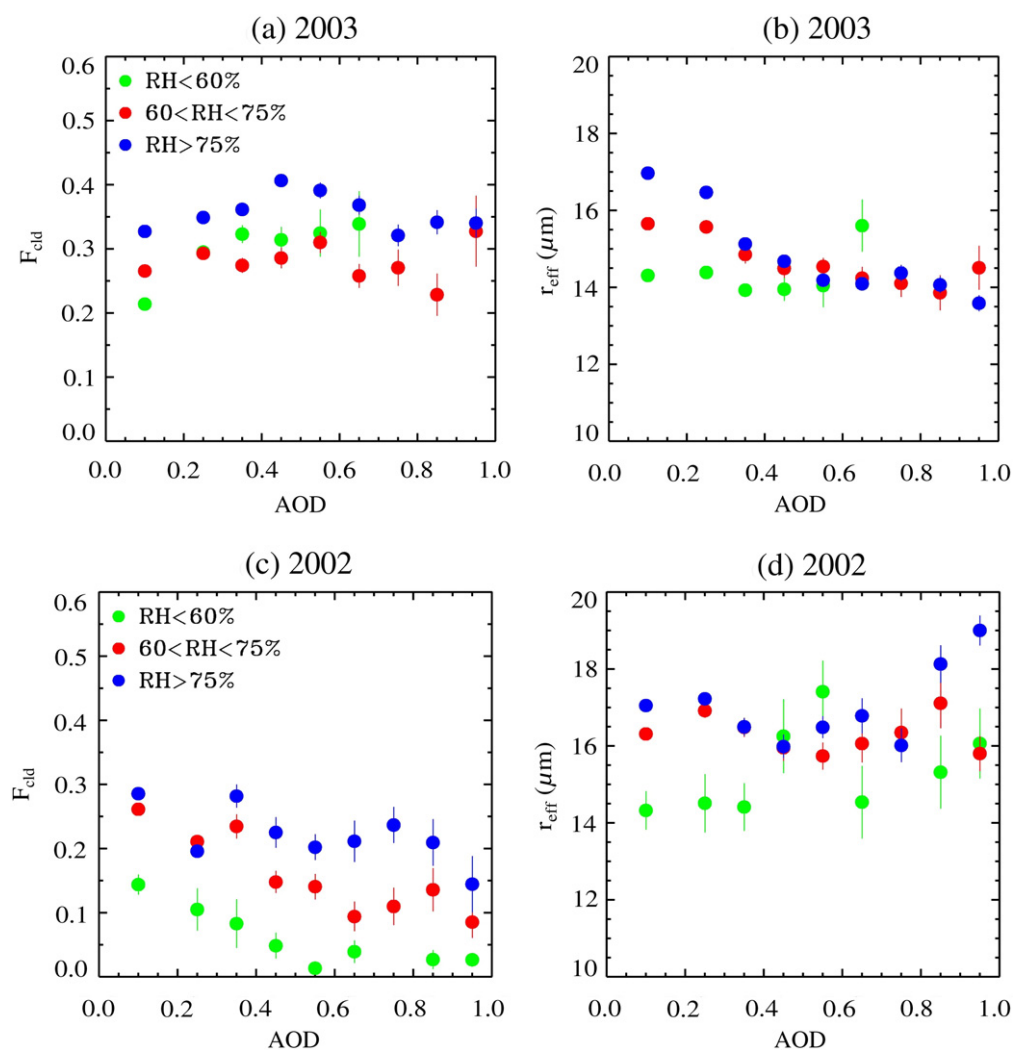


Fig. 14. Changes of cloud fraction (F_{cld}) (a, c) and cloud-top effective radius (r_{eff}) (b, d) with aerosol optical depth (AOD) for 2003 (a, b) and 2002 (c, d). The data are stratified by the 850 mb relative humidity (RH) from the ECMWF reanalysis.

atmosphere was more stable (Fig. 13a) and clouds were optically thinner and less extensive in 2002 (Fig. 13b–d) than in 2003. These conditions are not as favorable for strong aerosol effect as CCNs on cloud particles size distribution as for unstable and thick cloud condition. The thinner and less extensive clouds in 2002 would result in less attenuation of solar radiation before reaching the smoke layer and hence more absorption of solar radiation by the smoke that is more likely to reduce cloud fraction.

3.3. Changes of smoke-cloud relationships with atmospheric conditions

To explore whether or not the difference of atmospheric dynamics and thermodynamics shown in Section 3.2 could be responsible for the different smoke-cloud relationships between 2003 and 2002, we stratify the MODIS data for various meteorological parameters, including the atmospheric boundary layer (ABL) RH, LI, and the vertical low-level wind-shear (LLWS). The RH at the 850 mb level is used to stratify the aerosol-cloud analysis as shown in Fig. 14. In 2003, cloud fraction increases as

AOD increases from 0.1 to 0.4 under high RH ($>75\%$, Fig. 14a). For lower RH ($<75\%$) and heavier aerosol loading (AOD >0.4), the change of cloud fraction with AOD is not evident. The decrease of cloud droplet size is also greater for higher RH (Fig. 14b) as expected. In 2002, no systematic change of cloud droplet size with AOD can be detected. The cloud fraction decreases, instead of increasing as it did in 2003, with increasing smoke, especially for $RH < 75\%$ (Fig. 14c).

How the aerosol-cloud relationships change with atmospheric stratification is shown in Fig. 15. In 2003, the cloud fraction increases as AOD increases from 0.1 to 0.4 for a less stable lower troposphere (LI <3 , Fig. 15a). Cloud droplet sizes decrease with AOD for the similar AOD range as in Fig. 15a for less stable atmosphere (LI <5). These aforementioned changes do not exist for a more stable lower troposphere (LI >5), presumably due to a weaker or complete absence of updrafts. In 2002 (Fig. 15c), the reduction of cloud fraction with AOD is generally larger for larger LI, thus more stable lower troposphere (i.e., red and blue dots), particularly when AOD is less than 0.7. No systematic changes of cloud droplet size with AOD can be detected (Fig. 15d).

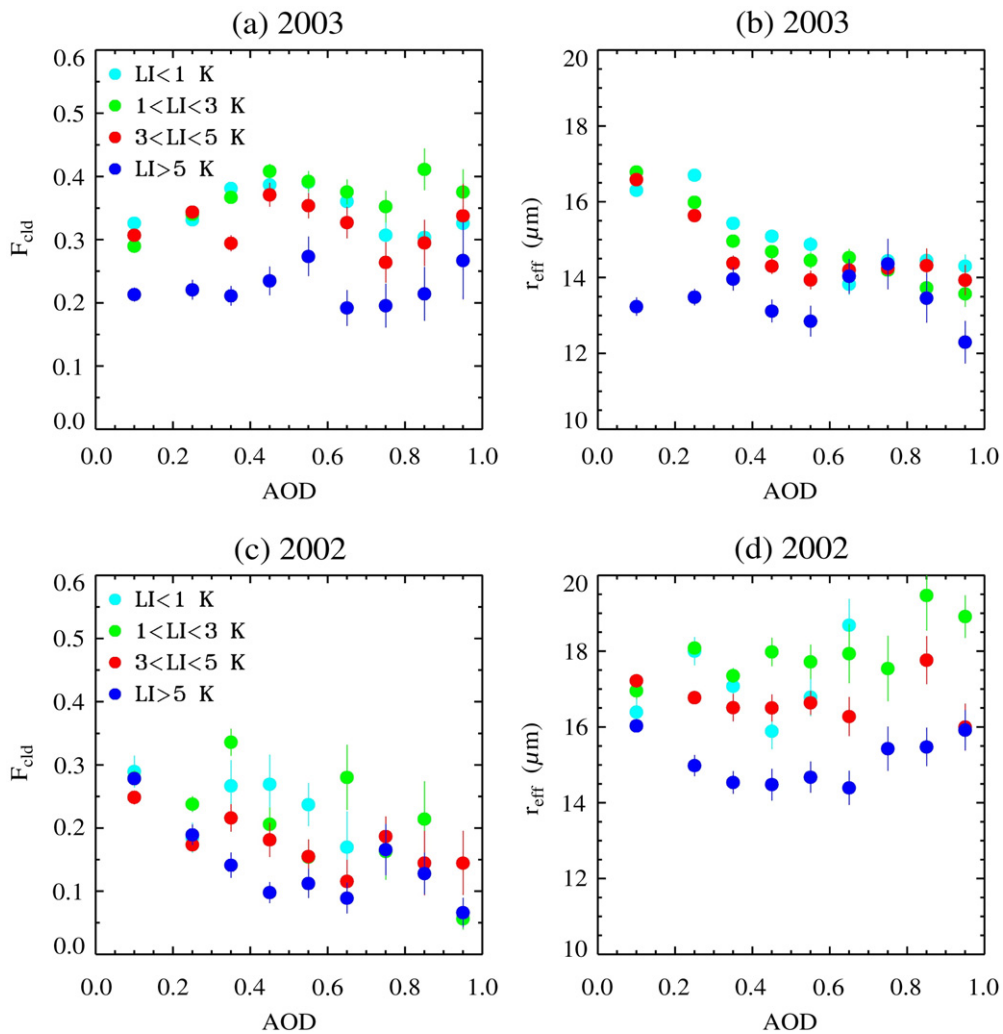


Fig. 15. Changes of cloud fraction (F_{cld}) (a, c) and cloud-top effective radius (r_{eff}) (b, d) with aerosol optical depth (AOD) for 2003 (a, b) and 2002 (c, d). The data are stratified by the MODIS-derived lifted index (LI).

Wind shear promotes and prolongs the development of clouds by their generation of turbulence and displacement of convective downdrafts (Liu & Moncrieff, 2001) and hence increases the cloud fraction. On the other hand, a strong wind shear may also shorten cloud lifetimes by promoting large lateral entrainment of dry ambient air into the cloud and decoupling of the cloud layer from the surface.

Fig. 16 examines how wind shear affects the relationship between smoke and clouds. The wind shear is defined here by a difference of horizontal wind speed between 925 mb and 700 mb (LLWS) (Peterson et al., 2002) as derived from radiosonde measurements over Manaus (3.15 °S, 59.98 °W), Brazil. The relation between cloud and aerosol in 2003 shows no clear dependence on the wind shear. In 2002, however, the cloud fraction decreases rapidly with increasing AOD for weaker vertical wind shear ($<2 \text{ m s}^{-1}$) as shown in Fig. 16c. For example, cloud fraction decreases from about 0.3 to 0.05 as AOD increases from 0.1 to 0.75. But for the stronger wind shear ($>2 \text{ m s}^{-1}$) cloud fraction changes little with AOD.

The above analyses generally indicate that the cloud fraction is reduced more for a lower troposphere with lower RH or a

more stability (higher LI), whereas cloud droplet size is reduced more and fraction increased more for a lower troposphere with higher RH or a less stability (lower LI). In addition, a weaker wind shear in a stable lower troposphere is associated with a stronger reduction of cloud fraction. However, deviations from such general relationships for individual parameters also exist. Such unexpected variability is presumably in part due to differences in aerosol properties and vertical structure, differences in sample sizes, uncertainties in the data we use, as well as other cloud and atmospheric conditions that cannot be included in our analysis due to lack of observations of these parameters.

4. Implications and discussion

4.1. What are the determining factors?

Both smoke aerosols and changes of meteorological conditions can change cloud fraction and droplet sizes. Determination of the underlying causes for observed changes of any smoke aerosol-cloud relationship requires that we establish whether or not: a) the observed aerosol-cloud

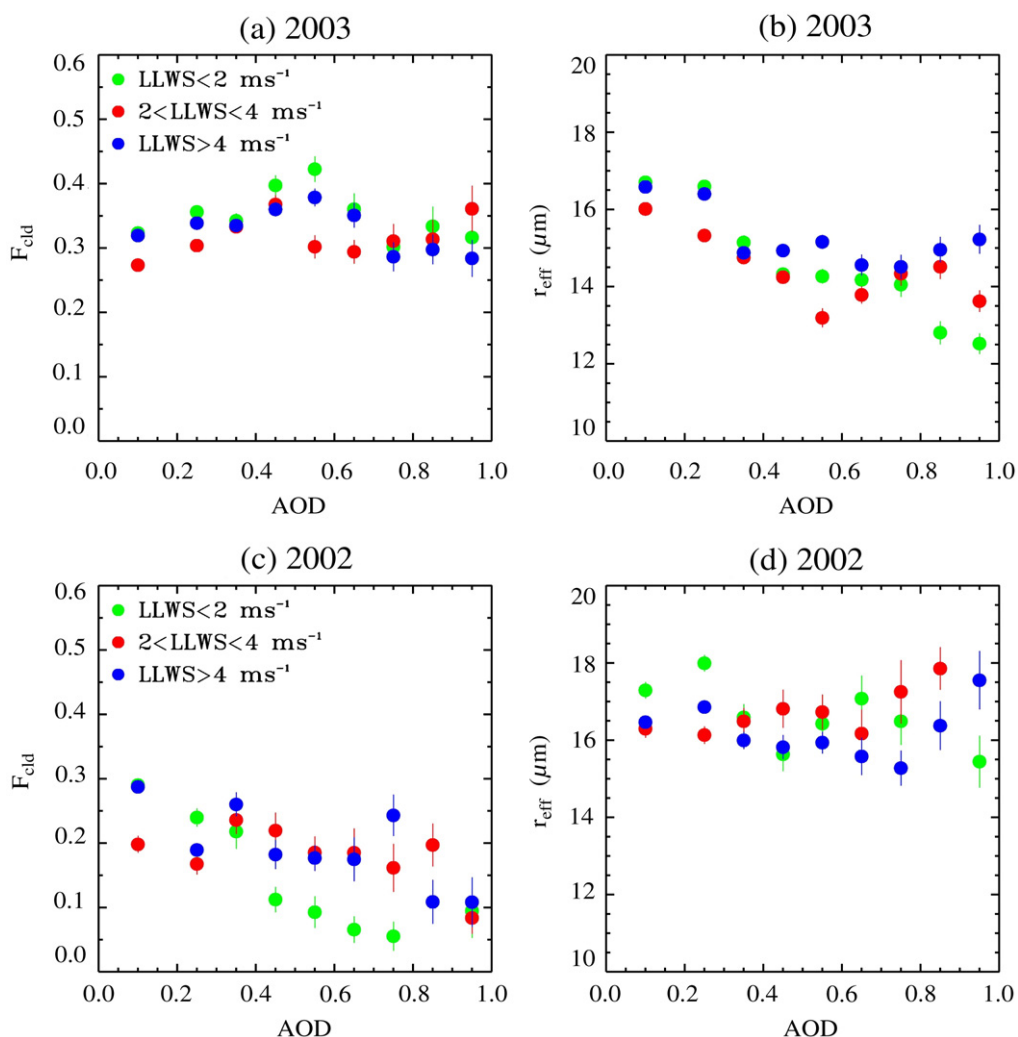


Fig. 16. Changes of cloud fraction (F_{cld}) (a, c) and cloud-top effective radius (r_{eff}) (b, d) with aerosol optical depth (AOD) for 2003 (a, b) and 2002 (c, d). The data are stratified by low-level wind difference between 925 and 700 mb as an index of vertical wind shear (LLWS) that is derived from radiosonde measurements over Manaus (3.15 °S, 59.98 °W), Brazil.

relationship is real and large compared to natural changes of cloud properties and meteorological conditions; b) that it is physically plausible; c) that there are no other alternative explanations for the observed relationship.

Why do we believe that the relationships are real? Cloud contamination in aerosol retrieval (Kaufman et al., 2005) or aerosol contamination in cloud retrieval (Brennan et al., 2005) could result in a positive correlation between cloud fraction and aerosol optical depth. As discussed earlier, the exclusion of the samples with high AOD and low cloud optical depth in our analysis should have minimized such artificial correlation between aerosol and cloud. While clouds cast shadows to reduce the reflected sunlight in the cloud neighboring regions, the reflection of sunlight from cloud sides can enhance the reflectance in the neighboring regions. Such an effect could introduce a high bias in retrieved AOD in the vicinity of clouds (Wen et al., 2006). Because this 3-D cloud effect increases with cloud cover, it could generate a spurious positive correlation between aerosol and cloud, especially for high cloud and AOD conditions. However, the positive correlation between cloud

fraction and AOD is weaker for higher AOD (>0.5) and cloud fraction than for lower AOD and cloud fraction (Fig. 5). Thus, this positive relationship cannot be explained by the 3-D cloud effects. In 2002, the cloud fraction decreased with increasing AOD. Such a relationship is opposite to those expected from those caused by retrieval errors.

Why do we believe the observed aerosols-cloud relationships are physically plausible? Our observations show that, when the lower troposphere is less stable and closer to saturation as it is during the transition season of 2003 (Figs. 10 and 12), the fraction of warm clouds increases with increasing LWP (Fig. 13). Higher LWP generally implies more well-developed thicker clouds associated with stronger updrafts. A stronger updraft can reduce the critical super-saturation for droplet growth, activating more aerosol particles or condensation nuclei (CN) into cloud condensation nuclei (CCN) and, hence, more effectively decreasing the droplet size given the same amount of available water (Feingold et al., 2003).

What are possible alternative explanations? The most obvious such possibility is that changes in the vertical distribution

of aerosols might have lead to the observed differences in cloud-aerosol relationships between the two years. Observations indicate differences in the vertical extent of the aerosol between the two years.

Aircraft measurements during the burning season of 2002 indicated that most of optically active aerosols were confined to the lowest 2000 m layer (Andreae et al., 2004; Chand et al., 2006). Space-borne lidar measurements from the Geoscience Laser Altimeter System (GLAS) launched in 2003 (Spinhirne et al., 2005) during September 25–November 19, 2003 (Fig. 17) show that most of smoke layers were confined to the lowest 2500 m layer. This suggests that the smoke layer was 500 m higher in 2003 than in 2002. Such a difference in the vertical distributions of aerosol may be associated with the less stable lower troposphere in 2003 than in 2002.

What might be the consequences of these observed differences? Some such consequences are entirely consistent with our previously presented hypothesis and some are not. The deeper smoke layer and higher cloud LWP in 2003 could provide more smoke particles for cloud condensation nuclei. Indeed, we have observed that cloud effective radii decrease and optical depth and fraction increase for warm clouds with higher LWP ($>40 \text{ g m}^{-2}$) as AOD increases from 0.1 to 0.4–0.6 and that clouds with similar LWP and top temperatures have optical depths and fraction that increase with AOD consistent with the radii decrease.

The impact of the smoke layer heating on meteorological conditions depends on the vertical distribution of the smoke. That is, solar absorption by smoke residing below cloud adds to the boundary layer heating in fueling convection, whereas at cloud level or above, it increases the inversion and stabilizes the atmosphere, as demonstrated by Yu et al. (2002), Feingold et al. (2005). In addition, the latter effect will increase with a greater AOD and so make the atmosphere drier, hence decreasing cloudiness.

We cannot determine how aerosol absorption would change between 2003 and 2002 based on the observations we have. Such a determination requires more reliable and comprehensive observation of the aerosol vertical distribution. However, the observation of a higher aerosol layer in 2003 suggests a greater stabilization. Thus, the deeper aerosol in 2003 apparently cannot explain the stronger increase of cloudiness with AOD seen in that year or to the absence of an observational relationship between cloud effective radii with AOD in 2002.

However, aerosol heating in the cloud layer could help amplify the effects of the already less saturated and more stable atmosphere in 2002 (Figs. 10–12), contributing to cloud dissipation, and consistent with the smaller fraction of clouds with lower LWP observed for 2002. The observed decrease of cloud fraction with AOD, especially for lower relative humidity and stronger stability (Figs. 14c and 15c), and the lack of systematic changes in cloud particle sizes (Figs. 14d and 15d) are consistent with clouds that are influenced by aerosol heating that stabilizes the lapse rate between surface and smoke layer.

Finally, even though the aerosol-cloud relationships are derived for similar atmospheric stability (LI) and RH conditions, the increase of atmospheric stability and decrease of RH

with AOD within each LI and RH category could still contribute to the observed decrease of cloud fraction with AOD. The contribution of this effect relative to the aerosol heating effect cannot be determined observationally.

Thus, our observations suggest that in the dry season of 2003 with its more unstable and humid atmospheric conditions, the dominant effect of aerosols was to decrease the sizes and increase the lifetimes of cloud droplets. On the other hand, in the corresponding period of 2002 with more stable and less saturated atmospheric conditions, stabilization by aerosol heating, or cloud “burning” appeared to be dominant. A contribution to these differences from a difference in the vertical profile of aerosol heating appears unlikely as in conflict with the observational evidence for a lower aerosol layer in 2002.

There are at least several additional factors that could in principle contribute to the observed changes in aerosol-cloud relationships that were not examined in this study. Kaufman and Koren (2006) showed that pollution and smoke aerosols could either increase or decrease the cloud cover, with a transition at aerosol absorption optical depth of about 0.05. This hypothesis might explain the shift from the increase to decrease of cloud fraction with increasing column aerosol concentration at AOD of about 0.5 in 2003 (Fig. 5). Does aerosol single-scattering albedo change from one year to another? Would such a change contribute to the changes in aerosol-cloud relationships? In a dry year like 2002, combustion would be more likely of a flaming phase, so besides being more frequent smoke would be darker. In contrast, in a wet year, higher fuel moisture would result in less absorbing smoke and fewer fires, hence fewer smoke soot particles. If so, the cloud fraction would decrease with increasing aerosol columnar concentration at a smaller AOD in 2002 than in 2003. Unfortunately, the limited number of observations cannot provide any conclusive assessment on this issue. For example, retrievals of aerosol single-scattering albedo (SSA) over two AERONET sites in the domain (Alta Florest and Abrocos Hill) suggest that smoke was even slightly darker (smaller SSA) in 2003 than in 2002, but the SSA

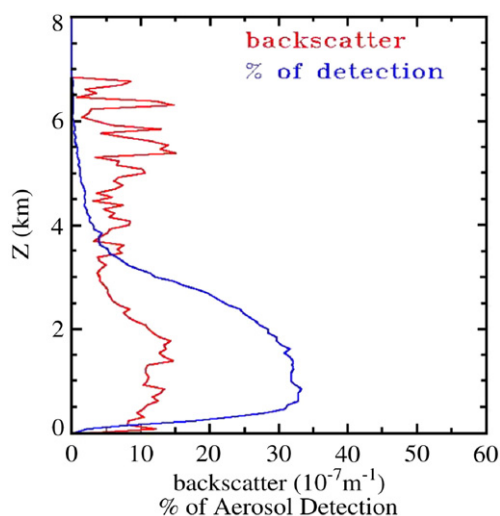


Fig. 17. Detection frequency of aerosol layers and the average aerosol backscatter measured by the Geoscience Laser Altimeter System (GLAS) during September 25–November 19, 2003.

difference of ~ 0.005 is much smaller than the uncertainty of 0.03 associated with SSA retrievals (Dubovik et al., 2002). It is also unclear whether smoke in 2002 was dark enough to be responsible for the decrease of cloud fraction with increasing aerosol loading at low AOD range as shown in Fig. 7 and in Koren et al. (2004). Any unambiguous attribution of the observed difference in the aerosol-cloud relationships to the difference in aerosol absorption properties remains difficult until more accurate measurements of aerosol absorption are available.

4.2. How would the interannual variation of aerosol-cloud interaction change radiative forcing?

What can we learn about the influence smoke aerosol on the radiation budget in the Amazon? Assuming that the observed change in aerosol-cloud relationships qualitatively represent the change of aerosol influence on warm clouds between 2003 and 2002, we can use a radiative transfer model (Fu et al., 1997) to provide a simple illustration as to how such a change might change the aerosol radiative forcing in the Amazon. Robust quantification of smoke forcing would require adequate measurements of aerosol and clouds and an estimate of uncertainties.

We use solar insolation of September 15 at 2.5 °S. The overall solar flux in the region is a fraction weighted average of clear-sky and cloudy-sky fluxes. Due to lack of observations, aerosol properties are assumed to be identical in the 2 years. The aerosol extinction is assumed to decrease with wavelength with an Angstrom exponent of 2 that is consistent with measurements by Chand et al. (2006). The aerosol single-scattering albedo and asymmetry factor are based on observations at two AERONET sites (Alta Florest and Abracos Hill) in the region (Dubovik et al., 2002). The single-scattering albedo of 0.93 at 550 nm is similar to that measured in situ (Chand et al., 2006). The asymmetry factor at 550 nm is 0.63. We assume that the aerosol is well mixed in the lowest 1700 m layer (Chand et al., 2006) and the same amount of aerosol as in the clear-sky is assumed to reside beneath the cloud layer. Cloud optical depth, droplet size, and cloud fraction are prescribed as functions of AOD from the correlation derived in this paper. Calculations are done for an AOD of 0.1 (background), 0.55 (“moderate smoke”), and 0.95 (“heavy smoke”). The background computation is subtracted from the moderate and heavy smoke computations to diagnose qualitatively the forcing by moderate and heavy smoke. The broadband surface albedo is taken from MODIS retrievals as 0.15 (Yu et al., 2004). Both instantaneous and 24-hour average forcings are estimated (the later with the same aerosol loading and smoke-cloud interactions during the day as that at 1:30 p.m.).

Fig. 18(a) and (b) show the calculated instantaneous (at 1:30 p.m.) smoke forcing and the 24-hour results, respectively. The 24-hour forcing is about 35% (for surface forcing) and 40–50% (for TOA forcing) of those at 1:30 p.m. Differences in the estimated aerosol forcing between the 2 years are largely determined by the observed different cloud fraction and aerosol relationships. Both surface and TOA aerosol forcing, defined by

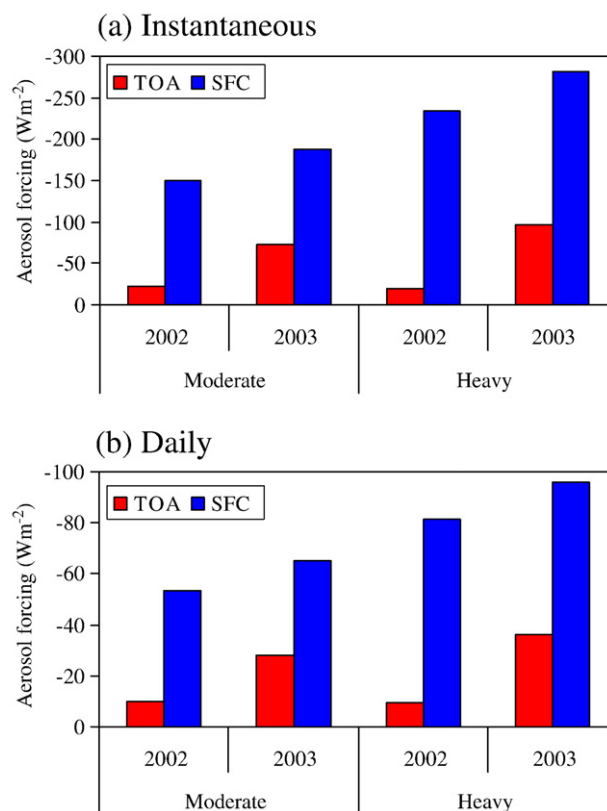


Fig. 18. Changes of (a) instantaneous (1:30 p.m. local time) and (b) daily solar radiative forcing at the top of atmosphere (TOA) and the surface for moderate (AOD=0.55) and heavy (AOD=0.95) smoke conditions and associated changes of warm clouds based on the aerosol-cloud relationship obtained from MODIS data. The aerosol single-scattering albedo and asymmetry factors are taken from AERONET measurements. The aerosol is assumed to be uniformly distributed in the lowest 2 km layer. Clear-sky and cloudy-sky fluxes are calculated separately and then weighted by clear-sky fraction and cloudy-sky fraction to derive average fluxes. For cloudy-sky calculations, the same amount of aerosol as in the clear-sky is assumed to present beneath the cloud layer. AOD=0.1 is an assumed background for deriving the aerosol forcing.

solar radiation reduction, are stronger in 2003 than in 2002, caused by increase of cloud fraction and optical thickness with aerosol in 2003. The aerosol forcing at TOA in 2002 is smaller as aerosol scattering is largely balanced by the decrease of cloud fraction. The atmospheric heating due to smoke absorption in 2002 is much stronger than in 2003 for moderate and heavy smoke conditions because of its greater fraction of clear-sky.

4.3. Potential influence on wet season onset over the Amazon

The increase of humidity in the ABL and weakening of the inversion are the primary conditions determining the dry-to-wet transition (Fu et al., 1999). The former depends on the soil moisture/vegetation conditions and surface solar flux during the early phase of the transition from dry to wet season (Li & Fu, 2004). Changes in land surface fluxes, as controlled by soil moisture and surface solar flux, are as important as the influence of ENSO in determining the interannual variations of wet season onset (Fu & Li, 2004). Our Fig. 18 suggests that the aerosol radiative forcing at the land surface is comparable to the

interannual changes of the land surface fluxes, thus could have significant influence on the transition from dry to wet season.

Finally, through numerical simulations, Yu et al. (2002) have suggested that the influences of aerosols on surface fluxes and ABL structure vary with soil moisture. Since local evapotranspiration is the primary source of the ABL moisture during dry and transition season (Li & Fu, 2004), the variation of aerosol-cloud relationship with relative humidity implies a significant role of land surface condition in determining the aerosol-cloud relationship.

5. Conclusions

An analysis of MODIS aerosol, warm cloud and lifted index retrievals, radiosonde profiles and the ECMWF reanalysis indicates very different smoke-cloud relationships between two different years. The differences appear to be largely correlated with atmospheric thermodynamic and moisture structure. In 2003, under wet and unstable atmospheric conditions and widely-spread thicker clouds, cloud droplet size decreased and cloud lifetime and fraction increased with increasing AOD except for low-level thin clouds. The decreased droplet sizes and increased cloud fractions can amplify the reflection of solar radiation by the smoke. In 2002, the atmosphere was drier and more stable than in 2003. The cloud fraction decreased with AOD for similar atmospheric stability and relative humidity conditions. No clear relationship between cloud effective radius and AOD could be detected, possibly because of too few samples for high LWP clouds. The reduction of cloudiness can compensate the effect of aerosol extinction on surface radiation balance. How aerosol absorption and its vertical distribution may have changed between the two years and hence possible effects cannot be assessed due to lack of high accuracy measurements.

Caution should be exercised when generalizing results about aerosol radiative forcing from any individual year to climatology. Our analysis implies effects of smoke on clouds could vary between a wetter and drier year. Changes in aerosol-cloud relationships can be generally explained by changes in meteorological conditions between the peak biomass burning seasons in 2002 and 2003, but whether changes in composition or absorption and vertical distributions of aerosols could also contribute to the changes in aerosol-cloud relationship still needs to be clarified. Analysis of more wet versus dry years is needed to determine whether our results can be generalized. Finally, extension of the results in this study to aerosols from the burning of African savannah or boreal forest would also be problematic because biomass burning smoke aerosols may have quite different physical and optical properties in these different regions (Eck et al., 2003).

Acknowledgements

The study is supported by NASA projects GWEC-0000-0101, EOS/03-0409-0018, and NNG04GB89G. We are grateful to Drs. Yoram Kaufman, Graham Feingold, Ilan Koren, and Lorraine Remer for their helpful discussions and Ms. Susan

Ryan for the editorial assistance. Insightful comments from a reviewer are highly appreciated.

References

- Ackerman, A. S., Toon, O. B., Stevens, D. E., Heymsfield, A. J., Ramanathan, V., & Welton, E. J. (2000). Reduction of tropical cloudiness by soot. *Science*, *288*, 1042–1047.
- Albrecht, B. A. (1989). Aerosols, cloud microphysics, and fractional cloudiness. *Science*, *245*, 1227–1230.
- Andreae, M. O., Rosenfeld, D., Artaxo, P., Costa, A. A., Frank, G. P., Longo, K. M., et al. (2004). Smoking rain clouds over the Amazon. *Science*, *303*, 1337–1342.
- Brennan, J. I., Kaufman, Y. J., Koren, I., & Li, R. (2005). Aerosol-cloud interaction — Misclassification of MODIS clouds in heavy aerosol. *IEEE Transaction. Geoscience and Remote Sensing*, *43*(4), 911–915.
- Chand, D., Guyon, P., Artaxo, P., Schmid, O., Frank, G. P., Rizzo, L. V., et al. (2006). Optical and physical properties of aerosols in the boundary layer and free troposphere over the Amazon basin during the biomass burning season. *Atmospheric Chemistry and Physics*, *6*, 2911–2925.
- Charlson, R. J., Seinfeld, J. H., Nenes, A., Kumula, M., Laaksonen, A., & Facchini, M. C. (2001). Atmospheric science: Reshaping the theory of cloud formation. *Science*, *292*, 2025–2026.
- Conant, W., Nenes, A., & Seinfeld, J. (2002). Black carbon radiative heating effects on cloud microphysics and implications for the aerosol indirect effect — 1. Extended Kohler theory. *Journal of Geophysical Research*, *107*(D21), 4604. doi:10.1029/2020JD002094
- Dubovik, O., Holben, B. N., Eck, T. F., Smirnov, A., Kaufman, Y. J., King, M. D., et al. (2002). Variability of absorption and optical properties of key aerosol types observed in worldwide locations. *Journal of Atmospheric Sciences*, *59*, 590–608.
- Dusek, U., Frank, G. P., Hildebrandt, L., Curtius, J., Schneider, J., Walter, S., et al. (2006). Size matters more than chemistry for cloud-nucleating ability of aerosol particles. *Science*, *312*, 1375–1378.
- Eck, T. F., Holben, B. N., Reid, J. S., O'Neil, N. T., Schafer, J. S., Dubovik, O., et al. (2003). High aerosol optical depth biomass burning events: A comparison of optical properties for different source regions. *Geophysical Research Letters*, *30*, 2035. doi:10.1029/2003GL017861
- Feingold, G., Eberhard, W., Veron, D., & Previdi, M. (2003). First measurements of the Twomey indirect effect using ground-based remote sensors. *Geophysical Research Letters*, *30*(6), 1287. doi:10.1029/2002GL016633
- Feingold, G., Jiang, H., & Harrington, J. Y. (2005). On smoke suppression of clouds in Amazonia. *Geophysical Research Letters*, *32*, L02804. doi:10.1029/2004GL021369
- Feingold, G., Remer, L. A., Ramaprasada, J., & Kaufman, Y. J. (2001). Analysis of smoke impact on clouds in Brazilian biomass burning regions: An extension of Twomey's approach. *Journal of Geophysical Research*, *106*, 22907–22922.
- Fu, R., & Li, W. H. (2004). The influence of the land surface on the transition from dry to wet season in Amazonia. *Theoretical and Applied Climatology*, *78*(1), 97–110. doi:10.1007/s00704-004-0039-6
- Fu, Q., Liou, K. -N., Cribb, M. C., Charlock, T. P., & Grossman, A. (1997). Multiple scattering parameterization in thermal infrared radiative transfer. *Journal of Atmospheric Sciences*, *54*, 2799–2812.
- Fu, R., Zhu, B., & Dickinson, R. E. (1999). How does the atmosphere and land surface influence seasonal changes of convection in the tropical Amazon? *Journal of Climate*, *12*, 1306–1321.
- Hastenrath, S., & Heller, L. (1977). Dynamics of climate hazards in northeast Brazil. *Quarterly Journal of the Royal Meteorological Society*, *103*, 77–92.
- Hobbs, P. V., Reid, J. S., Kotchenruther, R. A., Ferek, R. J., & Weiss, R. (1997). Direct radiative forcing by smoke from biomass burning. *Science*, *275*, 1776–1778.
- Jiang, H., Feingold, G., & Cotton, W. R. (2002). Simulations of aerosol-cloud-dynamical feedbacks resulting from entrainment of aerosol into the marine boundary layer during the Atlantic Stratocumulus Transition Experiment. *Journal of Geophysical Research*, *107*, 4813. doi:10.1029/2001JD001502
- Johnson, B. T., Shine, K. P., & Forster, P. M. (2004). The semi-direct effect: Impacts of absorbing aerosols on marine stratocumulus. *Quarterly Journal of the Royal Meteorological Society*, *130*, 1407–1422.

- Kaufman, Y., & Fraser, R. (1997). The effect of smoke particles on cloud and climate forcing. *Science*, 277, 1636–1639.
- Kaufman, Y. J., & Koren, I. (2006). Smoke and pollution aerosol effect on cloud cover. *Science*, 313, 655–658.
- Kaufman, Y., & Nakajima, T. (1993). Effect of Amazon smoke on cloud microphysics and albedo — Analysis from satellite imagery. *Journal of Applied Meteorology*, 32, 729–744.
- Kaufman, Y. J., Remer, L. A., Tanré, D., Li, R. -R., Kleidman, R., Mattoo, S., et al. (2005). A critical examination of the residual cloud contamination and diurnal sampling effects on MODIS estimates of aerosol over ocean. *IEEE Transactions on Geoscience and Remote Sensing*, 43(12), 2886–2897.
- Kaufman, Y. J., Tanré, D., Remer, L. A., Vermote, E. F., Chu, A., & Holben, B. N. (1997). Operational remote sensing of tropospheric aerosol over land from EOS moderate resolution imaging spectroradiometer. *Journal of Geophysical Research*, 102, 17051–17067.
- King, M. D., Menzel, W. P., Kaufman, Y. J., Tanre, D., Gao, B. -C., Platnick, S., et al. (2003). Cloud and aerosol properties, precipitable water, and profiles of temperature and water vapor from MODIS. *IEEE Transactions on Geoscience and Remote Sensing*, 41(2), 442–458.
- Koren, I., Kaufman, Y. J., Remer, L. A., & Martins, J. V. (2004). Measurements of the effect of Amazon smoke on inhibition of cloud formation. *Science*, 303, 1342–1345.
- Leitch, W. R., Banic, C. M., Isaac, G. A., Couture, M. D., Liu, P. S. K., Gultepe, I., et al. (1996). Physical and chemical observations in marine stratus during the 1993 North Atlantic Regional Experiment: Factors controlling cloud droplet number concentrations. *Journal of Geophysical Research*, 101, 29123–29135.
- Li, W., & Fu, R. (2004). Transition of the large-scale atmosphere and land surface conditions from dry to wet season over Amazon. *Journal of Climate*, 17, 2637–2651.
- Liu, Y., & Daum, P. H. (2002). Indirect warming effect from dispersion forcing. *Nature*, 419(10), 580–581.
- Liu, C., & Moncrieff, M. W. (2001). Cumulus ensembles in shear: Implications for parameterization. *Journal of Atmospheric Sciences*, 58, 2832–2842.
- Lohmann, U., & Lesins, G. (2003). Comparing continental and oceanic cloud susceptibilities to aerosols. *Geophysical Research Letters*, 30(15), 1791. doi:10.1029/2003GL017828
- Marshak, A., Platnick, S., Varnai, T., Wen, G., & Cahalan, R. F. (2006). Impact of three-dimensional radiative effects on satellite retrievals of cloud droplet sizes. *Journal of Geophysical Research*, 111, D09207. doi:10.1029/2005JD006686
- Matsui, T., Masunaga, H., Pielke, R. A., & Tao, W. (2004). Impact of aerosols and atmospheric thermodynamics on cloud properties within the climate system. *Geophysical Research Letters*, 31(6), L06109. doi:10.1029/2003GL019287
- Nakajima, T., King, M. D., Spinhirne, J. D., & Radke, R. F. (1991). Determination of the optical thickness and effective particle radius of clouds from reflected solar radiation measurements, part II: Marine stratocumulus observations. *Journal of Atmospheric Sciences*, 48, 728–750.
- Nenes, A., Charlson, R. J., Facchini, M. C., Kulmala, M., Laaksonen, A., & Seinfeld, J. H. (2002a). Can chemical effects on cloud droplet number rival the first indirect effect? *Geophysical Research Letters*, 29, 1848. doi:10.1029/2002GL015295
- Nenes, A., Conant, W., & Seinfeld, J. (2002b). Black carbon radiative heating effects on cloud microphysics and implications for the aerosol indirect effect — 2. Cloud microphysics. *Journal of Geophysical Research*, 107(D21), 4605. doi:10.1029/2020JD002101
- Penner, J. E., Dickinson, R. E., & O'Neill, C. A. (1992). Effects of aerosol from biomass burning on the global radiation budget. *Science*, 256, 1432–1434.
- Peterson, W. A., Fu, R., Chen, M. X., & Blakeslee, R. (2006). Intra-seasonal forcing of convection and lightning activity in the southern Amazon as function of cross-equatorial flow. *Journal of Climate*, 19, 3180–3196.
- Peterson, W., Nesbitt, S. W., Blakeslee, R. J., Cifelli, R., Hein, P., & Rutledge, S. A. (2002). TRMM observations of intraseasonal variability in/over the Amazon. *Journal of Climate*, 15, 1278–1294.
- Platnick, S., King, M. D., Ackerman, S. A., Menzel, W. P., Baum, B. A., Riedi, J. C., et al. (2003). The MODIS cloud products: Algorithms and examples from Terra. *IEEE Transactions on Geoscience and Remote Sensing*, 41(2), 459–473.
- Platnick, S., & Valero, F. (1995). A validation of a satellite cloud retrieval during ASTEX. *Journal of Atmospheric Sciences*, 52, 2985–3001.
- Procopio, A. S., Artaxo, P., Kaufman, Y. J., Remer, L. A., Schafer, J. S., & Holben, B. N. (2004). Multiyear analysis of Amazonian biomass burning smoke radiative forcing of climate. *Geophysical Research Letters*, 31, L03108. doi:10.1029/2003GL018646
- Rawlins, F., & Foot (1990). Remotely sensed measurements of stratocumulus properties during FIRE using the C130 aircraft multi-channel radiometer. *Journal of Atmospheric Sciences*, 47, 2488–2503.
- Reid, J. S., Hobbs, P. V., Rangno, A. L., & Hegg, D. A. (1999). Relationships between cloud droplet effective radius, liquid water content, and droplet concentration for warm clouds in Brazil embedded in biomass smoke. *Journal of Geophysical Research*, 104, 6145–6153.
- Remer, L. A., Kaufman, Y. J., Tanré, D., Mattoo, S., Chu, D. A., Martins, J. V., et al. (2005). The MODIS aerosol algorithm, products and validation. *Journal of Atmospheric Sciences*, 62(4), 947–973.
- Roberts, G., Nenes, A., Seinfeld, J., & Andreae, M. (2003). Impact of biomass burning on cloud properties in the Amazon Basin. *Journal of Geophysical Research*, 108, 4062. doi:10.1029/2001JD000985
- Rosenfeld, D. (1999). TRMM observed first direct evidence of smoke from forest fires inhibiting rainfall. *Geophysical Research Letters*, 26, 3105–3108.
- Rosenfeld, D., & Lansky, I. (1998). Satellite-based insights into precipitation formation processes in continental and maritime convective clouds. *Bulletin of the American Meteorological Society*, 79, 2457–2476.
- Salomonson, V. V., et al. (1989). MODIS, advanced facility instrument for studies of the earth as a system. *IEEE Transaction on Geoscience and Remote Sensing*, 27, 145–153.
- Schwartz, S. E., Harshvardhan, & Benkovitz, C. M. (2002). Influence of anthropogenic aerosol on cloud optical properties and albedo shown by satellite measurements and chemical transport modeling. *Proceedings of the National Academy of Sciences of the United States of America*, 99, 1784–1789.
- Sekiguchi, M., Nakajima, T., Suzuki, K., Kawamoto, K., Higurashi, A., Rosenfeld, D., et al. (2003). A study of the direct and indirect effects of aerosols using global satellite data sets of aerosol and cloud parameters. *Journal of Geophysical Research*, 108(D22), 4699. doi:10.1029/2002JD003359
- Sherwood, S. (2002). A microphysical connection among biomass burning, cumulus clouds, and stratospheric moisture. *Science*, 295, 1272–1275.
- Silva Dias, M. A., Rutledge, S., Kabat, P., Silva Dias, P. L., Nobre, C., Fisch, G., et al. (2002). Clouds and rain processes in a biosphere-atmosphere interaction context in the Amazon Region. *Journal of Geophysical Research*, 107, 8072. doi:10.1029/2001JD000335
- Spinhirne, J. D., Palm, S. P., Hart, W. D., Hlavka, D. L., & Welton, E. J. (2005). Cloud and aerosol measurements from the GLAS space borne lidar: initial results. *Geophysical Research Letters*, 32, L22S03. doi:10.1029/2005GL023507
- Tanré, D., Kaufman, Y. J., Herman, M., & Mattoo, S. (1997). Remote sensing of aerosol properties over oceans using the MODIS/EOS spectral radiances. *Journal of Geophysical Research*, 102, 16971–16988.
- Twomey, S. (1977). The influence of pollution on the shortwave albedo of clouds. *Journal of Atmospheric Sciences*, 34, 1149–1152.
- Wang, H., & Fu, R. (2002). Cross-equatorial flow and seasonal cycle of precipitation over South America. *Journal of Climate*, 15, 1591–1608.
- Wen, G., Marshak, A., & Cahalan, R. F. (2006). Impact of 3D clouds on clear sky reflectance and aerosol retrieval in a biomass burning region of Brazil. *IEEE Geoscience and Remote Sensing Letters*, 3, 169–172.
- Yu, H., Dickinson, R. E., Chin, M., Kaufman, Y. J., Holben, B. N., Geogdzhayev, I. V., et al. (2003). Annual cycle of global distributions of aerosol optical depth from integration of MODIS retrievals and GOCART model simulations. *Journal of Geophysical Research*, 108(D3), 4128. doi:10.1029/2002JD002717
- Yu, H., Dickinson, R. E., Chin, M., Kaufman, Y. J., Zhou, M., Zhou, L., et al. (2004). Direct radiative effect of aerosols as determined from a combination of MODIS retrievals and GOCART simulations. *Journal of Geophysical Research*, 109, D03206. doi:10.1029/2003JD003914
- Yu, H., Liu, S. C., & Dickinson, R. E. (2002). Radiative effects of aerosols on the evolution of the atmospheric boundary layer. *Journal of Geophysical Research*, 107(D12), 4142. doi:10.1029/2001JD000754